IEEE Access
Multidisciplinary | Rapid Review | Open Access Journal

Received February 14, 2019, accepted February 25, 2019, date of publication March 1, 2019, date of current version March 13, 2019.

Digital Object Identifier 10.1109/ACCESS.2019.2902195

Detection and Characterization of Mechanical Impact Damage Within Multi-Layer Carbon Fiber Reinforced Polymer (CFRP) Laminate Using Passive Thermography

YIN LI[1], AN-BO MING[1], HANG MAO[1], GUO-FENG JIN[1], ZHENG-WEI YANG[1], WEI ZHANG[1], AND SHAN-QI WU[2]

[1]Xi'an High-Tech Institute, Xi'an 710025, China
[2]8th Academy of China Aerospace Science & Industry Crop, Shanghai 201109, China

Corresponding author: An-bo Ming (mingab0628@163.com)

This work was supported by the National Natural Science Foundation of China under Grant 51575516 and Grant 51605481.

ABSTRACT With the increasing application of CFRP laminate, there is an 'urgent need for the rapid, visual, and non-intrusive method to 'detect mechanical impact damage. Passive thermography has been proven 'as a promising alternative to traditional nondestructive test technique by 'imaging the surface temperature difference of target with the advantages of 'real-time, non-intrusive, full-field, and visual 'results. Therefore, the aim of this paper is to 'characterize the impact damage types using passive thermography. To 'this goal, several specimens are subjected to impact test with 'different energies of 5, 10, 15, 20, '30, and 36 J and monitored by infrared camera. Then, active 'pulse thermography, SEM, and ultrasonic C-scanning are applied to 'detect the specimens respectively and the corresponding detection results 'are comparatively analyzed. On this basis, the impact damage 'types of CFRP are characterized. The obtained results show that 'different impact damage types occur under the different impact energies and 'can be characterized in the thermographic image. In detail, the 'matrix cracking, fiber rupture, and delamination can be characterized as 'hot spot with straight line shape along the fiber direction, hot spot 'with straight line shape perpendicular to the fiber direction and hot spot 'with irregular block shape respectively, which can facilitate the 'identification of impact damage mode and the evaluation of damage 'degree.

INDEX TERMS CFRP laminate, passive thermography, impact test, detection, characterization.

I. INTRODUCTION

CFRP composite laminate materials have been widely used for industrial applications, such as aerospace, automobile, wind energy and railway due to their excellent performances of high specific strength and stiffness, great designability, high fatigue resistance and strong corrosion resistance over many other types of materials [1].

However, the main weakness of CFRP composite materials is their low impact resistance; indeed, the CFRP composite materials are sensitive to the impact, caused by such mechanical impact sources as dropping tools, strong gales and stones, during manufacture, service and maintenance process. Generally, even a slight impact can induce the barely visible impact damage (BVID, i.e. damage not visible on the surface, but present in the internal), including matrix cracking, delamination, and fiber rupture, which can reduce the stiffness of structure, threatening the safety and reliability of structure [2]. Therefore, it is of significance to detect the mechanical impact damage in time to facilitate the subsequent repairs.

With respect to the impact damage detection, the available techniques can be summarized up for two categories: one is post-impacted detection technology, such as ultrasonic wave [3], radiography [4], microscopy [5], terahertz [6], etc., which are mainly used in the maintenance process for detecting damage after impact event to evaluate the structure integrity; while the other one, a real-time detection technology, is often used in the service process for structural health monitoring, such as acoustic emission [7], [8] and

The associate editor coordinating the review of this manuscript and approving it for publication was Bora Onat.

electro-mechanical impedance [9], which can gain the real-time information regarding to impact damage of materials. Although the above-mentioned methods have been proven successful for the impact damage detection of composite materials, a visual and non-intrusive method that is able to detect impact damage with high efficiency and reliability is needed.

With the development of optoelectronic technology, infrared thermography is viewed as a promising nondestructive detection method due to the advantages of high-speed, non-contact, large area inspection and visual results etc., which contains two approaches [10], [11]: active and passive during the thermography detections. In the active thermography detection, an external controllable stimulation source such as high energy pulse flash [12], power ultrasonic transducer [13], lock-in [14], [15], eddy current induced heating [16], microwave [17] and laser [18] is needed and applied to stimulate the thermal contrast of object. For this reason active thermography is generally used to detect the structures in the maintenance process as well as the detection methods described in [3]–[6], not suitable for the real-time detection. While the passive thermography [19]–[29] uses infrared camera to visualize temperature variations of an object without any external thermal stimulation, which demonstrates that this approach is suitable for the real-time detection.

With respect to passive thermography [19]–[22], it can satisfy the following demands: (i) real-time monitoring, (ii) rapid and visual detection, (iii) clean and non-contact, and (iv) large area coverage. On this account, many scholars have attempted some efforts on this method and its applications. As for the impact damage of composite materials, Meola and Carlomagno [23] used infrared camera to analyze the thermal effects of glass fiber reinforced polymer (GFRP) composite materials during impact events. Afterwards, the same phenomenon in the impact event of composite materials was also observed by Jakubczak *et al.* [24], which offered the possibility to assess the impact damage by passive thermography. Subsequently, Meola *et al.* [25]–[29] utilized this approach to detect impact damage of different composites materials (e.g. thermoset- and thermoplastic matrix composites), which was validated by active lock-in thermography and phased array ultrasonic. Additionally, as for the other mechanical damage of composite materials, Lai *et al.* [30] investigated the durability of FRP-concrete beams that were exposed to different conditions (i.e., elevated water temperatures of 25 °C, 40 °C and 60 °C for 5, 15, and 30 weeks) by using passive thermography to monitor the intermediate cracking processes under the quasi-static shear loading. Harizi *et al.* [11] evaluated the mechanical damage of glass fiber reinforced polymer (GFRP) composite laminates under static tensile loading by passive thermography and pointed that this method could detect some damages at high stress levels. In summary, passive thermography offers a promising alternative to traditional nondestructive test technique by imaging the surface temperature differences of objects that are subjected to the dynamic loading. However, to the best of our knowledge, how to characterize the impact damage types using passive thermography has been rarely involved yet.

Therefore, in this work, the mechanical impact damage of CFRP composite laminates was characterized. To this goal, the energy conversion during impact event was analyzed, which laid the foundation for the detection of impact damage of CFRP laminate using passive thermography. On this basis, several specimens are subjected to the impact test with different energies and monitored in real time by infrared camera. Finally, combined with active pulse thermography, SEM and ultrasonic C-scanning, the impact damage types are characterized by analyzing the thermographic images of specimens.

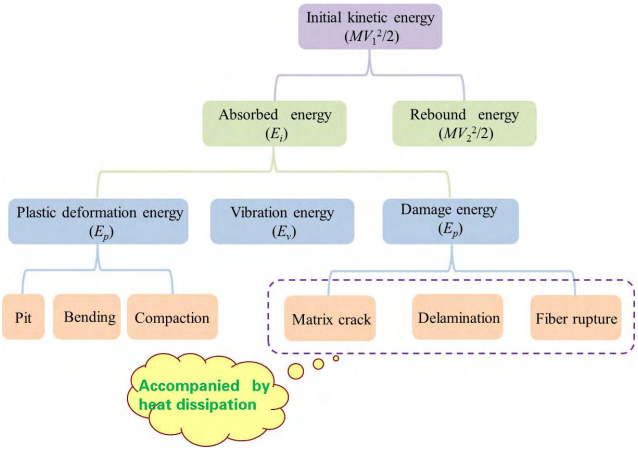

FIGURE 1. Energy conversion of specimen during impact event.

II. THEORETICAL FOUNDATIONS

During the impact event, the energy conversion of specimen is outlined in Fig. 1. Suppose that the pendulum head hits the specimen with a certain velocity, V_1, as a result, it is re-bounded by the specimen with another certain velocity, V_2, which is less than V_1. According to the energy balance equation proposed by Wang *et al.* [31] and Kang and Cheol [32] *et al.*, the loss kinetic energy, E_i, which is absorbed by the specimen, can be obtained as shown in Eq. (1).

$$E_i = \frac{1}{2}MV_1^2 - \frac{1}{2}MV_2^2 \tag{1}$$

where M is the mass of pendulum head, herein, the E_i is absorbed by specimen with threefold function as follows [31]:

$$E_i = E_p + E_v + E_d \tag{2}$$

where E_p is the plastic deformation energy, accounting for the pit, bending, and compaction deformation caused by impact; E_v is the vibration energy of specimen, accounting for the slight vibration of specimen after impact; E_d is the damage energy, accounting for the occurrence of matrix cracking, delamination and fiber rupture in the specimen.

Among the above three types of energy, both E_v and E_d are accompanied by heat dissipation. However, Kang and Cheol [32] pointed out that plastic deformation

energy E_p and damage energy E_d are the major energy absorption mechanisms for the impact event. For this reason E_v has a very small proportion in the absorbed energy and can be ignored. Thus, the heat dissipation can be considered as the production of E_d, which can lead to the surface temperature changes of specimen and pay the way for the detection of impact damage by measuring the variable temperature.

From infrared radiation framework, the surface temperature can be measured by infrared camera based on Planck's law [19], which lays the theoretical foundation for the variable temperature measurement using passive thermography.

III. EXPERIMENTAL DETAILS

A. MATERIALS AND EQUIPMENT

The studied specimens in this work are made of CFRP laminate, extended in $[45°/0°/-45°/90°]_{4s}$ and stacked in 32 layers with the size of 150 mm $\times$100 mm $\times$4 mm, which have been strictly carried out ex-factory detection using ultrasonic phased array technology to ensure the integrality.

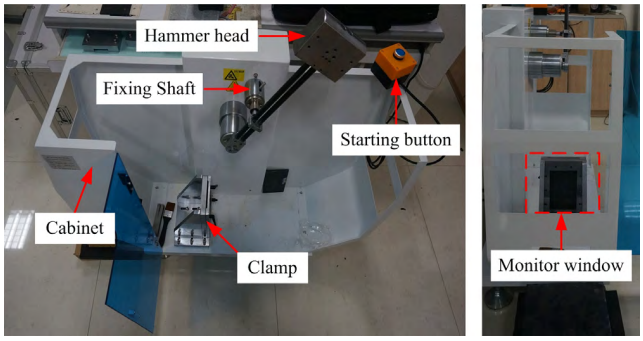

FIGURE 2. Impact devices and monitoring window. (a) Impact devices. (b) Monitoring window.

Fig. 2 shows the self-designed impact test device. In Fig. 2(a), the stainless pendulum head is used to hit the specimen, in which the load sensor and acceleration sensor are installed to gather the correlative data such as contact force, velocity et al and some threaded holes are prefabricated to add or reduce the stainless steel block to change the weight of pendulum head for adjusting the impact energy. The impact energy is calculated by the kinetic energy of pendulum head. Obviously, the kinetic energy is transformed by the potential energy. Therefore, the heavier of pendulum head presents the higher impact energy; the fixing shaft herein is acted with twofold function: fixing the pendulum head before and after the impact test and determining the initial height of pendulum head; the clamp is used to fastness the specimen. Additionally, to prevent the impact induced slag to sputter around, the impact device and clamp are placed in the cabinet.

The infrared camera is placed at the monitoring window, in Fig. 2 (b), to record the surface temperature field of specimen. The infrared camera used herein is produced by produced by Infra-Tec with the type of Vhr680, can detect the temperature range of -40 °C to 1200 °C with the sensitivity of 0.03 °C at 30 °C, accuracy of 2% of reading, resolution of 640 $\times$ 480 pixels, working in the infrared band range of 7.5-14 μm and maximal data capture rate of 50 frames per second.

In active pulse thermography, two high energy flash lamps are acted as the pulse stimulation source. The maximum energy of each lamp is 2.4 kJ with the stimulating interval of thermal wave of 2 ms. The SEM device, with the type of VEGA II XM, is used for the SEM testing, which can amplify the specimen by 4-100000X with the resolution of 3.0 nm. The ultrasonic C-scanning testing device, with the type of Rapid Scan 2, is produced by SONATEST and equipped with the wafer probe of 5L128-I2 that can emit and receive the ultrasonic wave with frequency of 5 MHz.

B. EXPERIMENTAL PROCEDURES

As indicated, this work focuses on the impact damage detection and characterization of CFRP laminate using passive thermography by measuring the surface temperature. We utilize the pendulum impact device in Fig. 2 to simulate the external impact source. The impact test is carried out using at the room temperature of 23° and the humidity of 30%. During the impact process, the infrared camera is placed at the monitor window in Fig. 2 (b) to implement the real-time monitoring and the corresponding procedure details are listed as the following five steps.

Step 1: Coating a thin layer of soluble black paint on the specimen surface to improve the infrared radiation rate and fixing the specimen in the clamp.

Step 2: Starting up the infrared camera, adjusting the focal distance to facilitate recording the clear thermal image sequence of specimen and conducting non-uniformity correction of infrared camera.

Step 3: To record the surface temperature change of specimen before and after the impact event, and conduct comparative analysis, recording and saving the thermal image sequence of specimen at some time before the falling off of pendulum head. Then, pressing the startup button to make the pendulum head fall off from the fixing shaft and hit the specimen. When rebounded, the pendulum head is man-made controlled to prevent multiple impacts on the specimen.

Step 4: changing the weight of pendulum head to adjust the impact energy and repeating the above three steps. In this work, several specimens with the number of #1-#6, are subjected to the impact test with different energies of 5 J, 10 J, 15 J, 20 J, 30 J and 36 J.

Step 5: detecting all the tested specimens using the active pulse thermography, SEM and ultrasonic C-scanning respectively.

It is worth noting that the recording image frames and recording frequency should be set suitable to record the whole heat dissipation process, to avoid the massive thermal image data storage and to facilitate the subsequent thermal image process. For these reasons, the gathered image frames are set

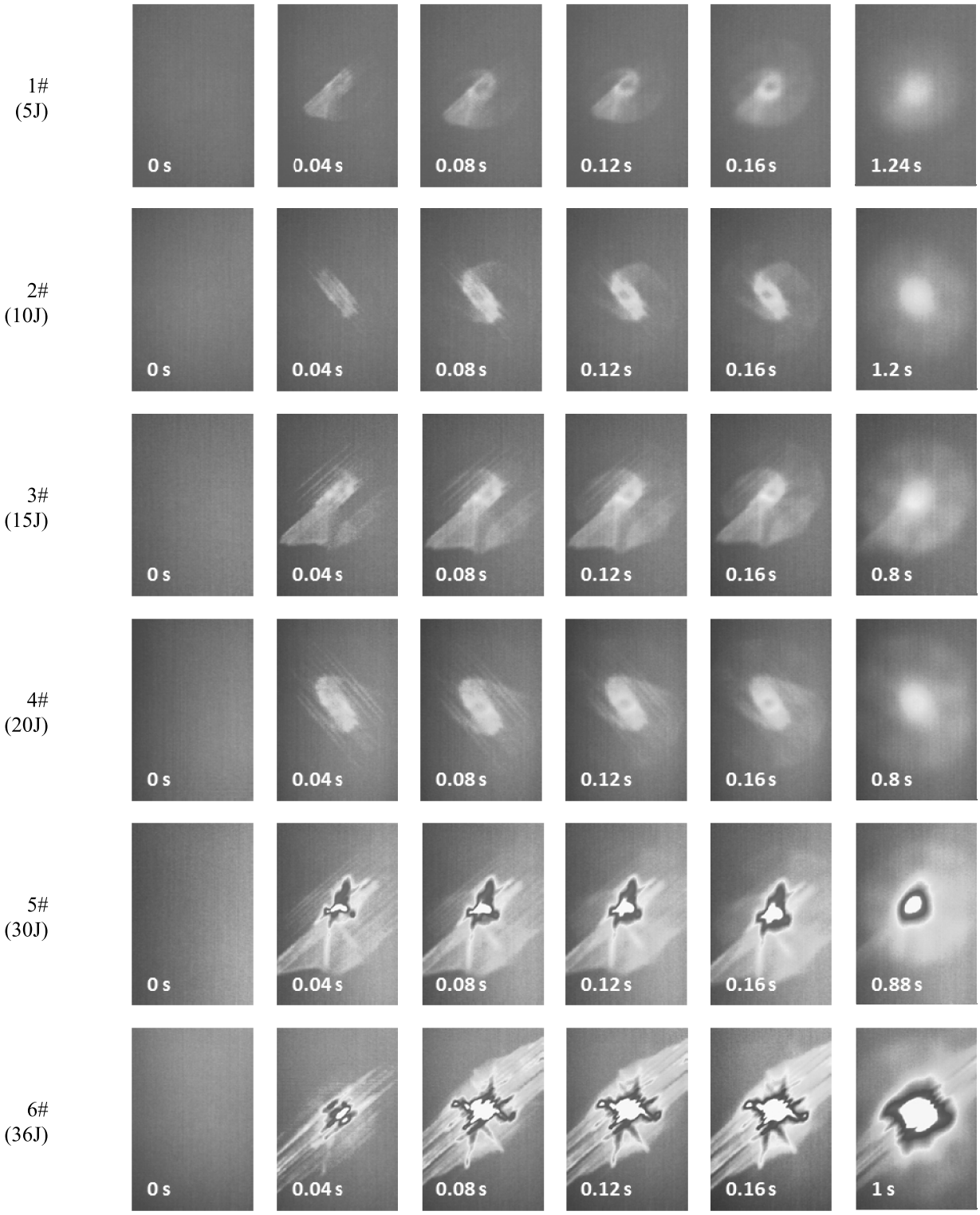

FIGURE 3. Thermal image sequence recorded by infrared camera.

of 800 and the recording frequency is set at 25 Hz, i.e., each frame of thermographic image is gathered every 0.04 s and total gathering time is 32 s in the passive thermography. The experimental details are listed in table 1.

IV. EXPERIMENTAL RESULTS

A. DETECTION RESULTS USING PASSIVE THERMOGRAPHY

The variable surface temperature is measured during impact event using infrared camera and the corresponding

TABLE 1. Experimental details.

Specimens	Impact energy (J)	Recording frequency (Hz)	Gathered frames
#1	5	25	800
#2	10	25	800
#3	15	25	800
#4	20	25	800
#5	30	25	800
#6	36	25	800

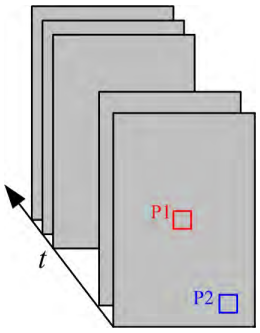

FIGURE 4. The selected area in the thermographic image sequence.

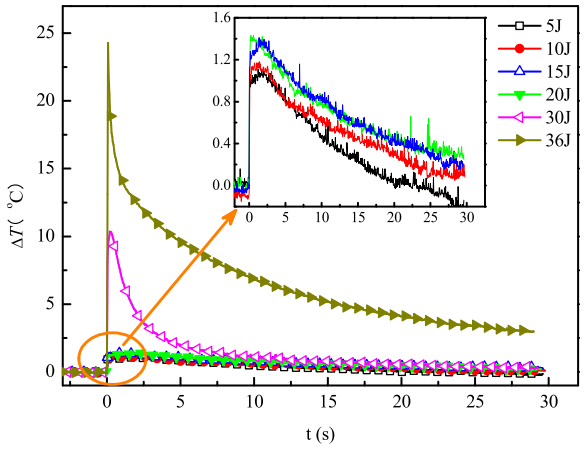

FIGURE 5. Surface temperature evolution curves of specimens.

thermographic image sequence of specimens with different energies are shown in Fig. 3.

In Fig. 3, due to the impact induced heat dissipation, the temperature of the hot spot in the impact area is higher than that of sound area, which can be used to locate the impact damage. Additionally, some valuable phenomena can be found and analyzed from the image sequence, listed as follows.

1) When t = 0 s, the pendulum head does not hit the specimen yet, thus there is no presence of hot spot in the thermographic image; even so, the surface temperature of the specimens shows different (i.e., there is the presence of highlight area and dark area on the specimen surface) because of the environment interfere and the surface characteristics of specimen, etc. in a complex manner. Then, the hot spot along the fiber layer direction (seems to matrix cracking) appears

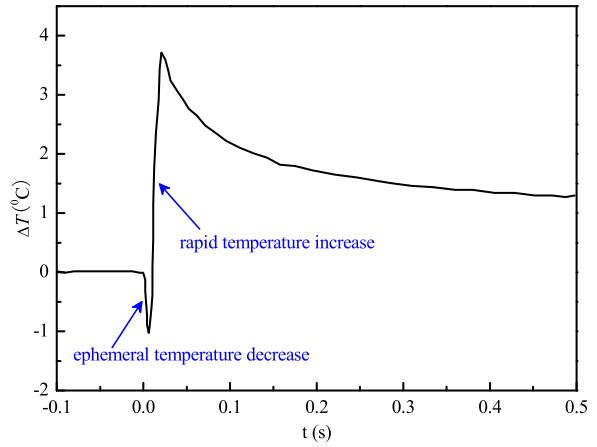

FIGURE 6. The ephemeral temperature decrease in the impact event in [23], [25], and [26].

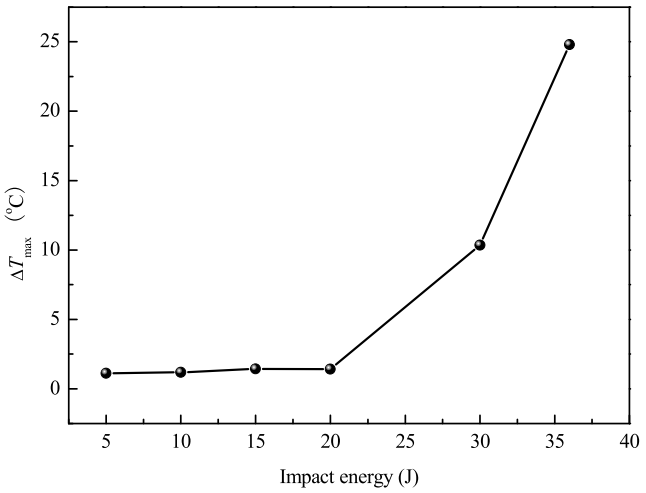

FIGURE 7. ΔT_{max} of specimens under different impact energies.

firstly with a straight line shape at t = 0.04 s. Afterwards, the hot spot starts to expand in a spiral manner (seems to delamination), till to form a circular hot spot at 0.16 s.

2) For a given impact energy, e.g. the image sequence of specimen #1 with impact energy of 5 J, the hot spot nearby the impact point is brighter than that of elsewhere, indicating temperature herein is higher, which may be due to the stress concentration and the occurrence of matrix cracking and delamination induced by impact event.

3) The hot spot with higher impact energy is brighter than that with lower impact energy at the same moment. Because the impact damage is more serious under the higher impact energy, as a result, the more heat is dissipated and leads to the higher surface temperature of specimen.

4) In the image sequence of specimens #1-#4, there is the presence of a relative dark point in the center of hot spot and the reasons are mainly derived from that impact induced pit leads to the reduction of thickness and the increase of the local density, according to the equation, $\alpha = k/\rho c$, the corresponding thermal diffusion efficiency, α, decreases with the increase of density, ρ, as a result, the ability to tend to heat

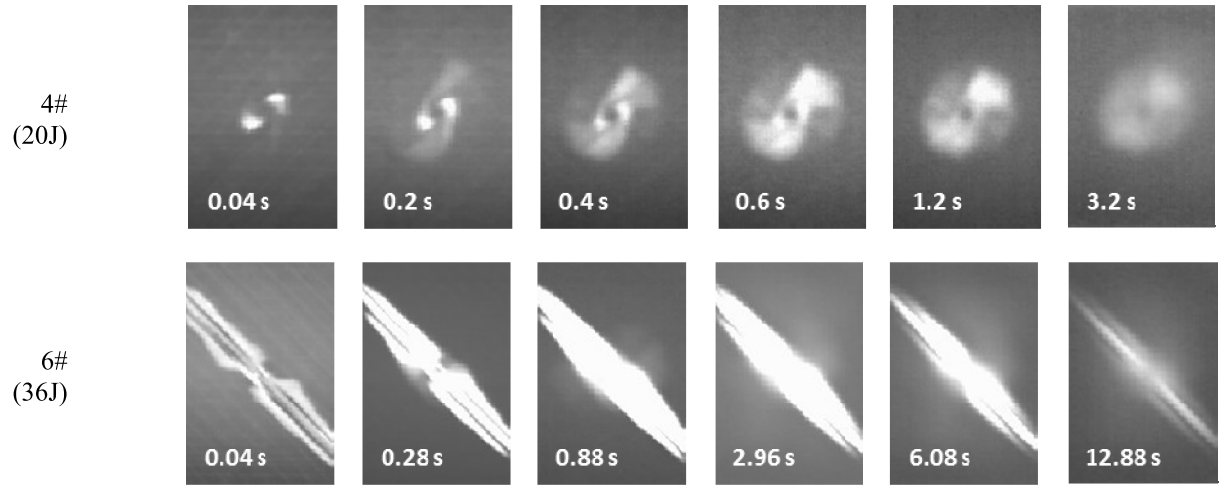

FIGURE 8. Partial detection results using active pulse thermography.

balance declines. While in the image sequence of specimens #5-#6, no dark point but brighter hot spot (e.g. white spot) appears, which indicates that the dissipated heat increases sharply under impact energy from 20 J to 30 J. The reason leading to this phenomenon is related with the occurrence of fiber rupture that releases abundant heat under larger impact energy (30 J and 36 J).

The occurrence of impact damage is accompanied by heat dissipation, which leads to the variable temperature on the specimen surface. Therefore, surface temperature analysis can facilitate the understanding of impact damage characterization. On this account, the surface temperature data is analyzed. To removing the influences of environment interfere and the surface characteristics of specimen on the surface temperature, the temperature difference, ΔT [26], is used in this work to investigate the variable temperature, which can be calculated using Eq. (3).

$$\Delta T_t = T_t - T_0 \tag{3}$$

where, T_t and T_0 are the surface temperature at the time of t and 0 respectively, and ΔT_t is the temperature difference at the time of t.

Two areas named P1 and P2 are selected in the damage area and sound area respectively and ΔT presents the subtraction of the mean temperature between P1 area and P2 area. The curves of ΔT vs. t of specimens with different impact energies is obtained using Eq. (3), as shown in Fig. 5. The ΔT remains unchanged with the value of 0 °C at $t < 0$ s, when the pendulum head does not hit the specimen. Whereas, the ΔT suddenly increases at t > 0 s when the pendulum head hits the specimen to release heat and then the ΔT gradually decreases due to the heat exchange with ambient environment, which is consistent with the phenomenon 1) described in section IV-A and the results in [23] and [25]–[29]. Herein, it is worth to point out that there is no presence of the phenomenon of ephemeral temperature decrease in this work but observed in [23], [25], and [26], as shown in Fig. 6. Meola and Carlomagno [25] explained that the ephemeral ΔT decrease phenomenon is present since the specimen surface reacts to the impact in an elastic manner (thermo-elastic effect) and the rapid ΔT increase phenomenon is due to the plastic reaction of specimen to impact event (thermo-plastic effect).

Compared with the ΔT curve in Fig. 6, the ΔT curve obtained in this work (in Fig. 5) only shows the rapid temperature increase phenomenon, not the ephemeral temperature decrease because the impact time is circa a few milliseconds while the gather frequency is set as 25 Hz, which is far slowly than that in [23], [25], and [26] of a few hundred hertz and leads to the loss of observation of the thermo-elastic effect. Nevertheless, the obtained results with relative slow gather frequency in this work may not seriously affect the detection of impact damage and characterization of impact damage types.

To explore the temperature changes under different impact energies, maximum surface temperature different, $\Delta T_{\max}$, between P1 area and P2 area is plotted against impact energy in Fig. 7.

From Fig. 7, we can find that when the impact energy is less than 20 J, the $\Delta T_{\max}$ increases relative smoothly but less than 1.5 °C, while when the impact energy reaches to 30 J and 36 J, the $\Delta T_{\max}$ reaches to 10 °C and 24 °C respectively, which indicates the $\Delta T_{\max}$ shows a nonlinear relationship with impact energy. In detail, there may be the presence of strong increase of $\Delta T_{\max}$ under some impact energy between 20 J and 30J, which is consistent with phenomena 3) and 4) in section IV-A and the reason may be relative with the change of impact damage types, i.e., the main impact damage types are matrix creaking and delamination when the impact energy is less than 20 J while the fiber breakage occurs and

accompanies with abundant heat dissipation when the impact energy reaches to 30 J and 36 J.

B. DETECTION RESULTS USING ACTIVE PULSE THEMOGRAPHY

According to the step 5 in section III-B, the specimens are detected using active pulse thermography and the thermal image sequence of partial specimens are shown in Fig. 8, in which the hot spot indicates the impact damage area.

Compared with the detection results using passive thermography, it can be found the similar and different phenomena in Fig. 8, which are described and analyzed as follows.

The similar phenomena contain two aspects: one is the whole process of appearance and spiral expansion of the hot spot (specimen 4#), which indicates there is impact damage in each sub-layer of the composite and demonstrates the impact damage is in possession of the characteristics of multi-level and multi-scale. The other is the presence of dark point in specimen 4# and brighter hot spot in specimen 6#, but the reason is different from that in passive thermography. In active pulse thermography, as for the specimen 4# with impact energy of 20 J, the reduction of thickness caused by impact event leads to the reduction of interspace between sub-layers, as a result, the capability of thermal impedance is weakened and few heat are cumulated, thus there is a dark point. While as for the specimen 6# with impact energy of 36 J, the occurrence of serious matrix cracking and fiber breakage on the surface of specimen (see Fig. 9 in section IV-C) in the impact event leads to the increase of interspace between sub-layers, as a result, the capability of thermal impedance is enhanced and abundant heat are cumulated, thus there is a brighter hot spot.

The different phenomenon is that the spiral expansion of the hot spot in specimen 6# is not observed and the reason is because serious surface matrix cracking and fiber breakage occur due to the impact and abundant heat are cumulated here, which may submerge the cumulated heat between sub-layers that are in the internal of specimen.

C. DETECTION RESULTS USING SEM AND ULTRASONIC C-SCANNING

Similarly, according to the step 5 in section III-B, the specimens are detected using SEM and ultrasonic C-scanning respectively and the corresponding partial results are shown in Fig. 9 and Fig. 10.

Fig. 9a shows the detection results of specimen 4# by amplifying by 100X, where we can find there is only the presence of matrix cracking that is along the direction of the fiber. Fig. 9b show the detection results of specimen 6# by amplifying by 55X, where we can find there is matrix cracking and fiber rupture. In fact, the occurrence of fiber rupture is generally accompanied with the matrix cracking because the fiber is wrapped by matrix in the composite

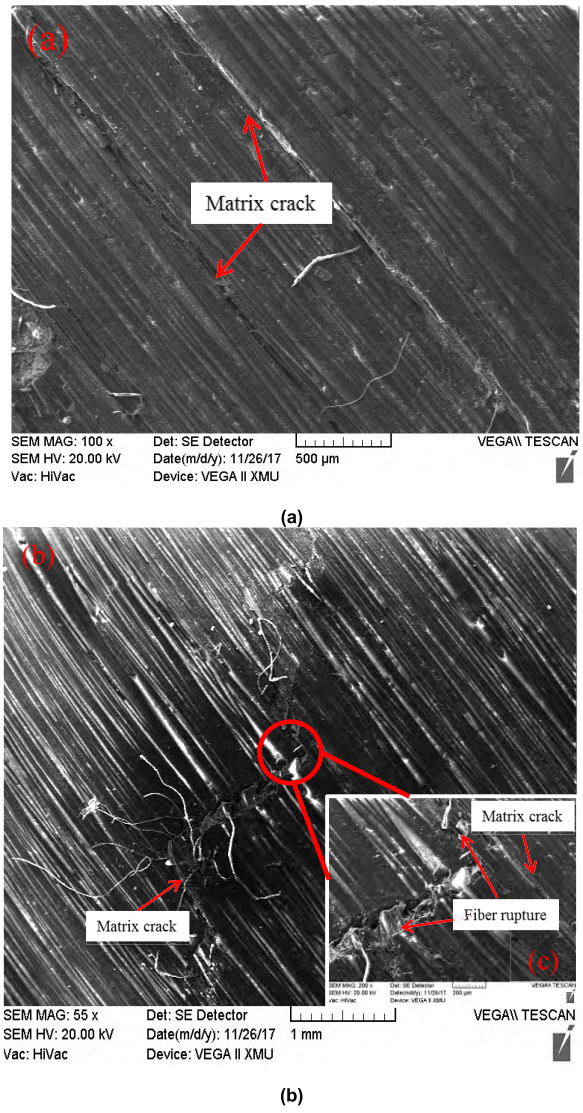

FIGURE 9. Partial results using SEM. (a) Specimen 4# magnified by 100 times. (b) Specimen 6# magnified by 55 times. (c) Specimen 6# magnified by 200 times.

structure and the strength of fiber is higher that of matrix. To further observing the fiber rupture, the results by amplifying by 200X are obtained in Fig. 9c, where we can find that the fiber rupture is perpendicular to the direction of the fiber. Additionally, there are explosion of fasciculi and shedding of colloid around the location of fiber rupture.

Fig. 10 shows the detection results of specimens 1#-4# using ultrasonic C-scanning, in which the delamination in the same sub-layer is displayed with the same color. From Fig. 10, we can find that there is delamination in each sub-layer and the area of delamination increases with increase of impact energy. Additionally, the delamination in each sub-layer shows the peanut shape, which is consistent with the results in [33]. Actually, the detection results of ultrasonic C-scanning show the superposition of delamination in each

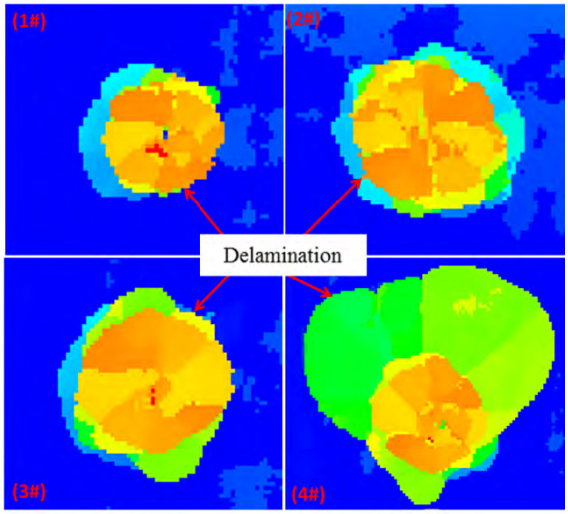

FIGURE 10. The detection results of specimen 1#∼4# using ultrasonic C-scanning.

sub-layer, thus, the delamination presents as a whole the irregular block shape.

D. IMPACT DAMAGE CHARACTERIZATION

In this section, the experimental results obtained by passive thermography, SEM and ultrasonic C-scanning are comprehensively analyzed to characterize the impact damage types.

From the above analysis, we can conclude that the matrix cracking and fiber rupture can be clearly detected using SEM and delamination can be clearly detected using ultrasonic C-scanning. Thus, the detection results obtained by SEM and by ultrasonic C-scanning are taken as references for the characterization of impact damage types.

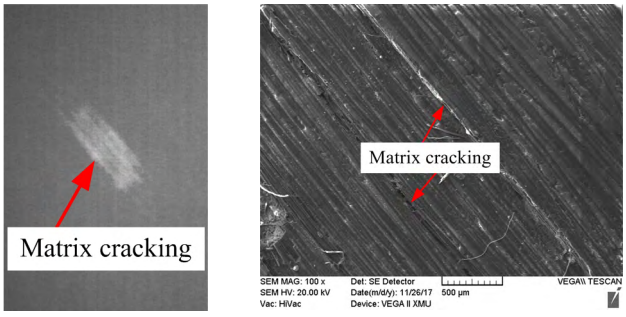

FIGURE 11. The morphology of matrix cracking.

The morphology profiles of matrix cracking, fiber rupture and delamination are shown in Figs. 11, 12 and 13 respectively.

From Fig. 11 and 12, taking the morphology profiles of matrix cracking and fiber rupture obtained by SEM as a reference, it can be deduced that the matrix cracking in passive thermography can be characterized as a straight hot spot along the fiber direction while the fiber rupture can be characterized as a straight hot spot perpendicular to fiber direction. Similarly, taking the morphology profile of delamination obtained by ultrasonic C-scanning as a reference in Fig. 13, it is

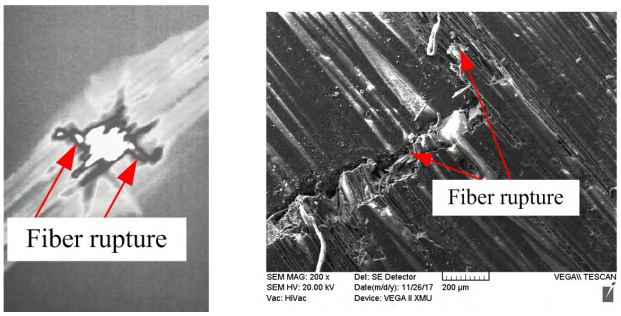

FIGURE 12. The morphology of fiber rupture.

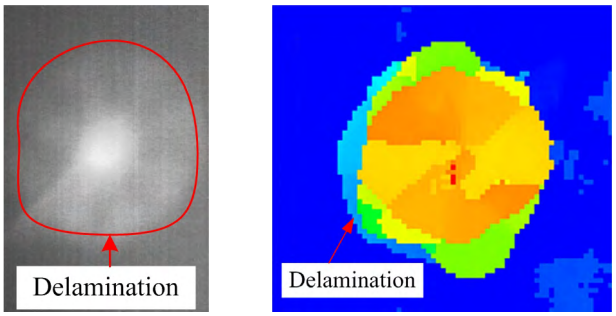

FIGURE 13. The morphology of delamination.

TABLE 2. Impact damage characterization in passive thermography.

Impact damage	Characterization in thermographic image
Matrix cracking	Hot spot with straight line shape along the fiber direction
Delamination	Hot spot with irregular block shape
Fiber rupture	Hot spot with straight line shape perpendicular to the fiber direction

deduced that the delamination can be characterized as a hot spot with irregular block shape.

In total, the characterization of impact damage types in passive thermography is listed in table 2.

V. DISCUSSION AND SUGGESTION

In literatures [23], [25]–[29], the scholars used passive thermography to detect impact damage at high frame rate. As a result, they have not only realized the real-time detection of impact damage, but also observed another significant phenomenon, i.e., thermo-elastic effect. Indeed, the impact process lasts very short, even several milliseconds. In this case, hundred hertz or thousand hertz frame rate can meet the demand of real-time detection of impact damage. Compared with the results obtained in these literatures, the results in this work with frame rate of 25 Hz indicate that the impact damage has been successfully detected with the advantages of high-speed, visualization and non-contact, and the impact damage types are characterized clearly in table 2, although the thermo-elastic effect phenomenon is missed at such low frame rate.

Compared with the detection results in Section IV A, B and C, we can sum up the strengths and weakness of passive

thermography, pulse active thermography, SEM and ultrasonic C-scanning. Passive thermography can observe the heat dissipation effect based on the energy conversation mechanism during impact process and realize the impact damage detection and characterization with the advantages of high-speed, visualization and non-contact. It also can detect the object with full field and locate the impact damage position accurately. But when the surface of object recovers thermal balance after impact process, this method cannot detect the impact damage even though there already is the presence of impact damage in the object. Pulse active thermography uses high energy flash lamp as external thermal excitation source and can detect the impact damage with the advantages of high speed, non-contact and large area inspection. However, it needs to further process the thermal image sequence due to the problems of uneven heating and reflection. SEM uses the high-power electron beam to scan the object surface to acquire the impact damage information. It can clearly observe the profile of impact damage that is on the surface of object while not detect the inner damage of object. Ultrasonic C-scanning is used to detect the impact damage based on high frequency wave propagation. It belongs to a contact detection method and needs coupling medium between the probe and object. It can detect the delamination in the object effectively but is not suitable for the detection of matrix cracking and fiber rupture. According to the analysis of strengths and weakness of these methods, a detection suggestion for the CFRP structures is proposed in this work as follows.

1) The infrared camera is used for monitoring the CFRP structures in service to real-time find the location of external mechanical impact damage.

2) The traditional nondestructive detection method, such as pulse active thermography and ultrasonic C-scanning, is applied to emphatically confirm the details of impact damage, which can facilitate the subsequent repairs of the structures.

VI. CONCLUSION

In this work, the aim is to characterize the impact damage types using passive thermography. To this goal, several specimens are firstly subjected to sharpy impact test with different energies and real-time detected using passive thermography, followed by detected using such nondestructive detection methods as active pulse thermography, SEM and ultrasonic C-scanning. Then, the detection results are comparatively analyzed to realize the characterization of impact damage types. The obtained results show that different impact damage types occur under the different impact energies. In detail, when the impact energy is low, the impact damage types contain matrix cracking and delamination, while the impact energy is large, in addition to the matrix cracking and delamination, the fiber rupture occurs. On this basis, Impact damage types are characterized in passive thermography. The matrix cracking and fiber rupture are characterized as hot spot with straight line shape along the fiber direction and perpendicular to the fiber direction, respectively, while the delamination can be characterized as hot spot with irregular block shape, which can facilitate the identification of impact damage mode and the evaluation of damage degree.

It is worth noting that this work is potentially to determine the relationship between the damage types and impact energies. However, more experiments are needed to find the threshold of energy between different damage types.

REFERENCES

[1] M. K. Bannister, "Development and application of advanced textile composites," *J. Mater. Des. Appl.*, vol. 218, no. 3, pp. 253–260, 2004.

[2] T.-W. Shyr and Y.-H. Pan, "Impact resistance and damage characteristics of composite laminates," *Compos. Struct.*, vol. 62, pp. 193–203, Nov. 2003.

[3] M. Castaings, D. Singh, and P. Viot, "Sizing of impact damages in composite materials using ultrasonic guided waves," *NDT & E Int.*, vol. 46, pp. 22–31, Mar. 2012.

[4] S. C. Garcea, Y. Wang, and P. J. Withers, "X-ray computed tomography of polymer composites," *Compos. Sci. Technol.*, vol. 156, pp. 305–319, Mar. 2018.

[5] M. S. Sohn, X. Z. Hu, J. K. Kim, and L. Walker, "Impact damage characterisation of carbon fibre/epoxy composites with multi-layer reinforcement," *Compos. B, Eng.*, vol. 31, no. 8, pp. 681–691, 2000.

[6] T. Chady, P. Lopato, and B. Szymanik, "Terahertz and thermal testing of glass-fiber reinforced composites with impact damages," *J. Sensors*, vol. 2012, Feb. 2012, Art. no. 954867. doi: 10.1155/2012/954867.

[7] N. Liu, Q. M. Zhu, C. Y. Wei, N. D. Dykes, and P. E. Irving, "Impact damage detection in carbon fibre composites using neural networks an acoustic emission," *Key Eng. Mater.*, vol. 167, pp. 43–54, Jun. 1999.

[8] M. Saeedifar, M. A. Najafabadi, D. Zarouchas, H. H. Toudeshky, and M. Jalalvand, "Clustering of interlaminar and intralaminar damages in laminated composites under indentation loading using Acoustic Emission," *Compos. B, Eng.*, vol. 144, pp. 206–219, Jul. 2018.

[9] T. Wandowski, P. H. Malinowski, and W. M. Ostachowicz, "Delamination detection in CFRP panels using EMI method with temperature compensation," *Compos. Struct.*, vol. 151, pp. 99–107, Sep. 2016.

[10] W. Harizi, S. Chaki, G. Bourse, and M. Ourak, "Mechanical damage assessment of polymer–matrix composites using active infrared thermography," *Compos. B, Eng.*, vol. 66, pp. 204–209, Nov. 2014.

[11] W. Harizi, S. Chaki, G. Bourse, and M. Ourak, "Mechanical damage assessment of glass fiber-reinforced polymer composites using passive infrared thermography," *Compos. B, Eng.*, vol. 59, pp. 74–79, Mar. 2014.

[12] K. Zheng, Y.-S. Chang, K.-H. Wang, and Y. Yao, "Improved nondestructive testing of carbon fiber reinforced polymer (CFRP) composites using pulsed thermograph," *Polym. Test.*, vol. 46, pp. 26–32, Sep. 2015.

[13] Y. He, S. Chen, D. Zhou, P. Wang, and S. Huang, "Shared excitation based nonlinear ultrasound and vibrothermography testing for CFRP barely visible impact damage inspection," *IEEE Trans. Ind. Informat.*, vol. 14, no. 12, pp. 5575–5584, Dec. 2018. doi: 10.1109/TII.2018.2820816.

[14] V. Arora, J. A. Siddiqui, R. Mulaveesala, and A. Muniyappa, "Pulse compression approach to nonstationary infrared thermal wave imaging for nondestructive testing of carbon fiber reinforced polymers," *IEEE Sensors J.*, vol. 15, no. 2, pp. 663–664, Feb. 2015.

[15] J. A. Siddiqui, V. Arora, R. Mulaveesala, and A. Muniyappa, "Infrared thermal wave imaging for nondestructive testing of fibre reinforced polymers," *Experim. Mech.*, vol. 55, no. 7, pp. 1239–1245, 2015.

[16] T. Liang, W. Ren, G. Y. Tian, M. Elradi, and Y. Gao, "Low energy impact damage detection in CFRP using eddy current pulsed thermography," *Compos. Struct.*, vol. 143, pp. 352–361, May 2016.

[17] A. Foudazi, I. Mehdipour, K. M. Donnell, and K. H. Khayat, "Evaluation of steel fiber distribution in cement-based mortars using active microwave thermography," *Mater. Struct.*, vol. 49, no. 12, pp. 5051–5065, Dec. 2016.

[18] T. Li, D. P. Almond, and D. A. S. Rees, "Measurement Science and Technology Crack imaging by scanning laser-line thermography and laser-spot thermography," *Meas. Sci. Technol.*, vol. 22, no. 3, pp. 407–414, 2011.

[19] S. Bagavathiappan, B. B. Lahiri, T. Saravanan, T. Jayakumar, and J. Philip, "Infrared thermography for condition monitoring—A review," *Infr. Phys. Technol.*, vol. 60, pp. 35–55, Sep. 2013.

[20] A. Rogalski, "Infrared detectors: An overview," *Infr. Phys. Technol.*, vol. 43, pp. 187–210, Jun. 2002.

[21] B. B. Lahiri, S. Bagavathiappan, T. Jayakumar, and J. Philip, "Medical applications of infrared thermography: A review," *Infr. Phys. Technol.*, vol. 55, pp. 221–235, Jul. 2012.
[22] A. Rogalski, "Recent progress in infrared detector technologies," *Infr. Phys. Technol.*, vol. 54, pp. 136–154, May 2011.
[23] C. Meola and G. M. Carlomagno, "Infrared thermography of impact-driven thermal effects," *Appl. Phys. A*, vol. 96, pp. 759–762, Aug. 2009.
[24] P. Jakubczak, J. Bieniaś, and B. Surowska, "Impact damage live-time analysis of modern composite materials using thermography," *Compos. Theory Pract.*, vol. 14, no. 4, pp. 219–223, 2014.
[25] C. Meola and G. M. Carlomagno, "Impact damage in GFRP: New insights with infrared thermography," *Compos. A, Appl. Sci. Manuf.*, vol. 41, pp. 1839–1847, Dec. 2010.
[26] C. Meola *et al.*, "New perspectives on impact damaging of thermoset- and thermoplastic-matrix composites from thermographic images," *Compos. Struct.*, vol. 152, pp. 746–754, Sep. 2016.
[27] C. Meola *et al.*, "Impact damaging of composites through online monitoring and non-destructive evaluation with infrared thermography," *NDT & E Int.*, vol. 85, pp. 34–42, Jan. 2017.
[28] C. Meola and G. M. Carlomagno, "Infrared thermography to evaluate impact damage in glass/epoxy with manufacturing defects," *Int. J. Impact Eng.*, vol. 67, pp. 1–11, May 2014.
[29] C. Meola, S. Boccardi, G. M. Carlomagno, N. D. Boffa, E. Monaco, and F. Ricci, "Nondestructive evaluation of carbon fibre reinforced composites with infrared thermography and ultrasonics," *Compos. Struct.*, vol. 134, pp. 845–853, Dec. 2015.
[30] W. L. Lai, S. C. Kou, C. S. Poon, W. F. Tsang, and K. K. Lee, "A durability study of externally bonded FRP-concrete beams via full-field infrared thermography (IRT) and quasi-static shear test," *Construct. Building Mater.*, vol. 40, pp. 481–491, Mar. 2013.
[31] Y. Wang, X. Zhang, and H. Wang, "Low-velocity impact response of composite laminate and its relationship with damage parameters," (in Chinese), *Chin. J. Solid Mech.*, vol. 34, no. 1, pp. 63–72, Feb. 2013.
[32] T. J. Kang and C. Kim, "Impact energy absorption mechanism of largely deformable composites with different reinforcing structures," *Fibers Polym.*, vol. 1, pp. 45–54, Mar. 2000.
[33] Y. Duan, W. Yao, and F. Chen, "A nonlinear mixed-mod model oriented low velocity impact damage of FRP," (in Chinese), *J. Nanjing Univ. Aeronaut. Astronaut.*, vol. 50, no. 1, pp. 16–23, Feb. 2018.

YIN LI was born in Jianyang, Sichuan, China. He received the B.S. degree in aircraft power engineering and the M.S. degree in aerospace science and technology from the Xi'an High-Tech Institute, Shaanxi, China, in 2012 and 2014, respectively, where he is currently a Research Assistant. Recently, he has published academic papers in famous international journals including *Composites Structures*, the *International Journal of fatigue*, *NDT & E International*, and *Infrared Physics & Technology*. His research interests include non-destructive testing and fault diagnosis.

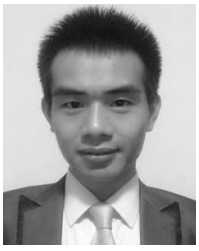

AN-BO MING was born in Luzhou, Sichuan, China. He received the B.S. degree in aircraft power engineering, in 2007, the M.S. degree in aircraft design, in 2010, and the Ph.D. degree in aerospace science and technology from the Xi'an High-Tech Institute, Shaanxi, China. From 2010 to 2014, he was a Visiting Ph.D. Candidate in mechanical engineering with Tsinghua University, Beijing, China. He is currently a Lecturer with the Xi'an High-Tech Institute, Shaanxi, China. His research interests include rolling element bearing fault diagnosis, signal processing, and bearing fault dynamics. He has chaired or participated more than ten projects including NFSC and Provincial Fund Project. He has published academic papers in famous international journals including *Mechanical Systems and Signal Processing* and the IEEE TRANSACTIONS ON INDUSTRIAL ELECTRONICS, especially the paper titled Dual-impulse Response Model for the Acoustic Emission Produced by a Spall and the Size Evaluation in Rolling Element Bearings has been published in the IEEE TRANSACTIONS ON INDUSTRIAL ELECTRONICS, vol. 62, no. 10, 2015.

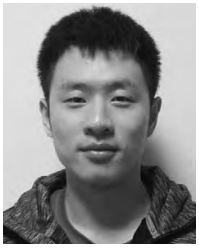

HANG MAO was born in Leshan, Sichuan, China. He received the B.S. degree in aircraft power engineering from the Xi'an High-Tech Institute, Shaanxi, China, in 2016, where he is currently pursuing the master's degree. His research interests include non-destructive testing and structural health monitoring. Recently, he has published some academic papers in a famous Chinese Journal *Noise and Vibration Control*.

GUO-FENG JIN was born in Luoyang, Henan, China. He received the B.S. degree in aircraft power engineering, the M.S. degree in environmental engineering, and the Ph.D. degree in aerospace science and technology from the Xi'an High-Tech Institute, Shaanxi, China, in 2006, 2009, and 2013, respectively, where he is currently a Lecturer. He has published more than 30 academic papers in journals and conferences and participated in more than ten projects. His research interests include non-destructive testing, structural health monitoring, and damage prognosis.

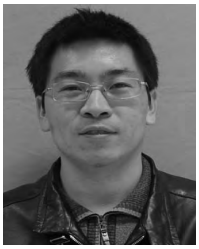

ZHENG-WEI YANG was born in Nanyang, Henan, China. He received the B.S. degree in aircraft power engineering, the M.S. degree in aviation engineering, and the Ph.D. degree in aerospace science and technology from the Xi'an High-Tech Institute, Shaanxi, China, in 2005, 2007, and 2011, respectively, where he is currently an Assistant Professor of aerospace science and technology. His research interests include non-destructive testing and structural health monitoring. He has published more than 50 academic papers in journals and conferences, chaired or participated more than ten projects and published two books titled *Thermography Testing and Quantitative Identification for Adhesive Structure of Solid Rocket Motor* and *Infrared Thermal Wave Testing and Images Sequence Processing Technology* (National Defense Industry Press in Chinese).

WEI ZHANG was born in Shanxian, Shandong, China. He received the B.S. degree in power machine from the Xi'an High-Tech Institute, Shaanxi, China, in 1985, the specialized M.S. degree in mechanics from Xi'an Jiaotong University, in 1995, and the Ph.D. degree in ordnance science and technology from the Xi'an High-Tech Institute, Shaanxi, China, in 2003, where he is currently a Professor of aerospace science and technology. His research interests include non-destructive testing, condition monitoring, and fault diagnosis. He has chaired or participated more than 50 projects including NSFC and Provincial key projects, held about five patents in china, published more than 80 academic papers in journals and conferences and four books in English or Chinese, especially the book title *Failure Characteristics Analysis and Fault Diagnosis for Liquid Rocket Engines* (Springer-Verlag Berlin Heidelberg Press). He is a Reviewer for about ten academic journals.

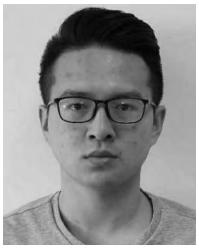

SHAN-QI WU was born in Baoji, Shannxi, China. He received the B.S. degree in automation engineering from Northwestern Polytechnical University, in 2012, and the M.S. degree in armament science and technology from the Xi'an High-Tech Institute, Shaanxi, China, in 2014. He is currently an Assistant Engineer with 8th Academy of China Aerospace Science & Industry Crop, Shanghai, China. His research interests include fault diagnosis and equipment maintenance.